The detection of gear noise computed by integrating the Fourier and Wavelet methods

NIOLA VINCENZO[1], QUAREMBA GIUSEPPE[1], FORCELLI ANIELLO[2]

[1]Department of Mechanical Engineering for Energetics
University of Naples "Federico II"
Via Claudio 21, 80125, Napoli
ITALY
vniola@unina.it http://niola.dime.unina.it

[2]DVH Transmission Department
ELASIS S.C.p.A.
Via ex Aeroporto, s.n. , 80038, Pomigliano d'Arco (NA)
ITALY

Abstract: - This paper presents a new gearbox noise detection algorithm based on analyzing specific points of vibration signals using the Wavelet Transform. The proposed algorithm is compared with a previously-developed algorithm associated with the Fourier decomposition using Hanning windowing. Simulation carried on real data demonstrate that the WT algorithm achieves a comparable accuracy while having a lower computational cost. This makes the WT algorithm an appropriate candidate for fast processing of noise gear box.

Key-Words: - Signal processing, gear noise, Wavelet Transform, multiresolution analysis.

1 Introduction

Gears are one of the most common and important machine components in many advanced machines. The most common method for gear noise assessment is subjective evaluations. Evaluators either drive the vehicle or listen to the tape on which the noise data was recorded to rank the noise. The subjective evaluations have some drawbacks. First of all, the subjective ratings are not consistent and may change from time to time. Secondly, the resolution of the ratings is limited by the auditor's ability to distinguish small difference in the gear noises. Additionally, the cost for conducting a subjective evaluation is much higher than for an objective one. Subjective evaluation often requires more people to be involved.
Noise and vibration properties of cars have become important criteria in the competition between automotive manufacturers and together with new legislation are an important reason to reduce noise and vibrations.
Moreover, noise and vibrations are seen as indicators of the quality of the product: noisy products create a "cheap" impression while silent products gives the impression of quality. Moreover, car manufacturers' demands, on one hand, to reduce the total vehicle weight and on the other hand, to increase power at lower speed. As a consequence noise due to the gearbox is expected to increase and to be less masked by the engine noise.
For this reason, this work deals with the objective measurement of the gear noise, in particular with the analysis of the gear whine which represents transmission noises resulting from gears engaged in the torque flow, *i.e.* teeth engagement noise.
In this paper we present results obtained by our basic noise research on the vibration of gears using a "traditional" Fourier approach compared to an "innovative" Wavelet approach.

2 The Problem

Many vehicle manufacturers, research and academic institutions have focused their attention on vehicle acoustic design. Noise emissions produced by the transmission play a significant role. In fact, transmission acoustic rating is one of the customer's acceptance criterion.
The most maddening vibrations are induced by the engagement impulse ($f = nz / 60$, n is the speed and z is the number of teeth). The greater the load, the more important the entity of this impulse is. The angular speed of the mating gears has a relevant influence too. Acoustic optimization has to find solutions that minimize such impulses.

Our research activities therefore have been planned according to the following development roadmap:

- 1st phase: noise generation *i.e.* teeth engagement
- 2nd phase: noise transfer *i.e.* gearbox housing and bearings
- 3rd phase: noise emission *i.e.* the transmission housing to the human perception.

Typically, to reduce the gear whine noise, two options are possible:

- optimization of the gear's macro-geometry *e.g.* using high contact ratio gears that leads to minor noise emissions in conjunction with higher transmitted power levels
- optimization of the gear's micro-geometry *e.g.* by trying to balance load-induced teeth deflections with profile corrections which generally leads to less noisy transmission effects. This is not a suitable solution for an overall working range; therefore profile corrections must be determined statistically to take into account manufacturing deviations which will overlap their effect.

This paper focused on the 1st phase. The goal is to find a method to process the data in order to find the teeth engagement discontinuity during the torque transmission which caused noise.
All the experimental activities are performed in Elasis using the Virtual Engine Simulator described in the next paragraph.

3 The automotive transmission tool

The Virtual Engine Simulator (VES) is the latest tool for automotive transmissions Noise Vibration and Harshness (NVH) testing. A view of a VES setup for testing and evaluating the gear noise is shown in Fig. 1.

Fig. 1. Virtual engine simulator

The major benefit of using VES in gear noise testing is its ability to reproduce engine output irregularities, therefore, gearboxes can be objectively evaluated and tested without the need to build their associated engines. This capability is extremely important in reducing the product time to market.
Since VES can accurately reproduce mean value of both speed and combustion and inertia forces, car manufactures are able, in this way, to test prototype gearbox earlier in the process, before prototype engines are available.
Fig. 2 shows a schematic diagram of the virtual engine simulator. As shown in this figure, unlike conventional test rigs, this particular virtual engine simulator has a mechanical coupling between the input dynamometer and a high performance dynamic pulse generator.

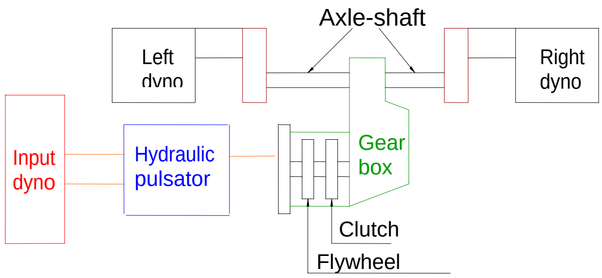

Fig. 2. Virtual engine simulator: schematics

In order to load the gearbox output shafts, each half-shaft is equipped with additional dynamometers to simulate road loads. The output dynamometers are sized to cover a wide range of vehicle speeds and torques. In addition to the simulated road loads, flywheels are installed on the output dynamometer to represent vehicle inertias.
The virtual engine simulator can be controlled by providing excitation time histories generated either by computer software (synthesized) or measured on a real vehicle.

4 The test-rig

As shown in Figure 3, the test-rig is installed in a semi anechoic chamber where dynamometers are soundproofed inside enclosures. In the same way, in order to achieve appropriate background conditions for gear noise measurements, the floor is covered with soundproofing material.

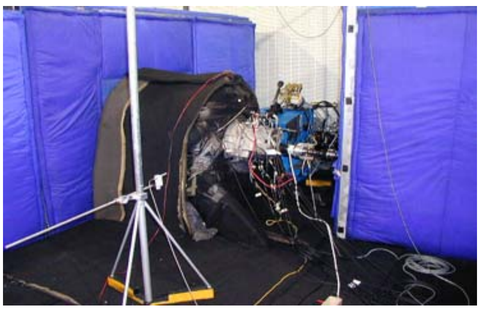

Fig. 3. Virtual engine simulator settled in semi anechoic chamber

Such a set-up, unlike what happens on the vehicle or in a power train test-cell, uncouples the noise generated by the gearbox from the other noises present on the vehicle or generated by the engine. For this reason, the noise problem is pronounced and consequently, noise investigation becomes easier and more objective.

The test rig is equipped with the following signals:

- engine shaft velocity fluctuation measured by magnetic sensors at the flywheel and at the primary shaft
- sound pressure level (SPL) measured by using capacitive microphones (sensitivity 0.051 V/Pa), located at one meter far from transmission housing
- piezoelectric accelerometers (sensitivity 1pC/ms-2) placed on the gearbox housings.

The gearbox oil temperature is also monitored because of the strong influence of the gear whine with the oil viscosity. All the tests are performed at 70°C.

A five-speed manual shifted transmission is used for the analysis presented in this paper. The time history acquired on the car is first recorded, during a wide-open throttle condition with the second gear engaged, and then it is reproduced on the test rig. The second gear is selected because it leads to very audible gear whine noise inside the vehicle cabin, especially up to 5500 round per minute (rpm).

5 Data processing and results

5.1 Fourier's method

The accelerometer used in this test has been placed on the gearbox housing (Fig. 4), in correspondence of the contact point of gears.

Fig. 4. Acceleration measure point

Fig. 5 shows the time history of the second gear for the engine speed (green, red) and accelerometer vibrations (blue).

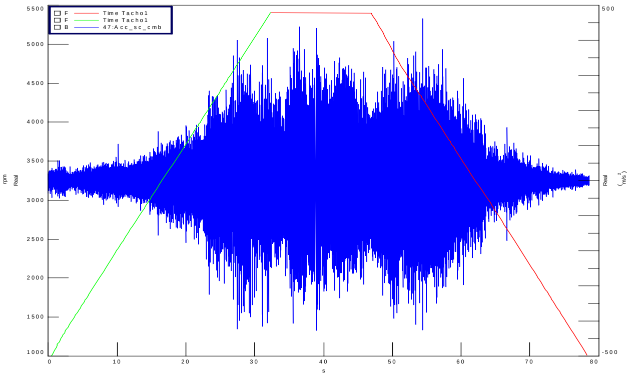

Fig. 5. Time history and vibrations

Duration of signals is roughly 80 seconds and it consists of one slow acceleration in 33 seconds, a stationary phase (12 seconds) and than a deceleration in 33 seconds.

The conversion from time-domain data to frequency domain is performed using the Fast Fourier Transform (FFT) [1] technique. In this application, where the engine speed is steadily increasing and decreasing (engine run up & run down case respectively), a family of FFT operations is obtained to scan the range of the engine speed of interest. Thus, two Campbell diagrams [2] have been created, one for the acceleration phase and the other for the deceleration phase.

Acquired signal has been processed with a sampling frequency of 51200 hz, using Hanning windowing [3] and a resolution of 25 rpm.

Figg. 6-7 show the contribution in frequency according to engine speed. In order to indicate the signal amplitude a chromatic scale is used.

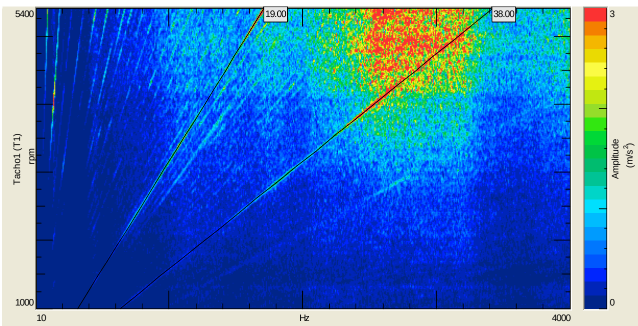

Fig. 6. Campbell diagram during acceleration phase

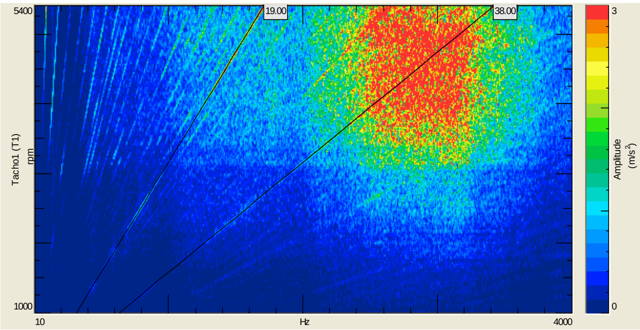

Fig. 7. Campbell diagram during deceleration phase

Spectral content is calculated to extract the overall levels and engagement orders for both run up and run down maneuvers.
The engagement orders are referred to:

- the gear order (order 19) and its first harmonic (order 38)
- the final reduction order (order 7.4)and its first harmonic (order 14.8).

Fig. 8 reports the order analysis for both acceleration and deceleration phase.

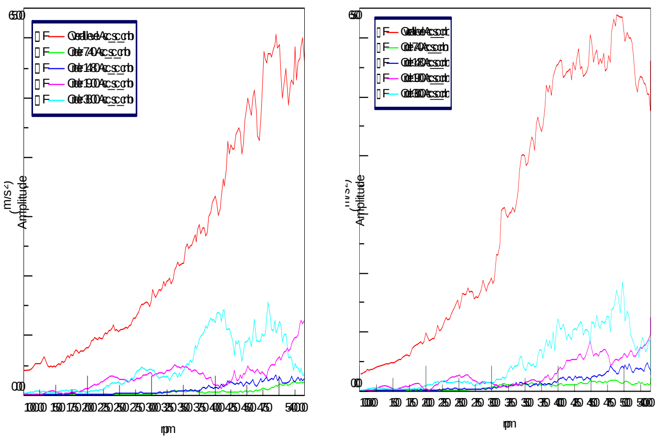

Fig. 8. overall level and engagement orders

5.2 The method of Wavelet Transform

In the following subsections we describe the main concepts regarding the Discrete Wavelet Transform.
The word wavelet is used in mathematics to denote a kind of orthonormal bases in L^2 with remarkable approximation properties.
Wavelets allow to simplify the description of a complicated function in terms of small number of coefficients. Often there are less coefficients necessary than in the classical Fourier analysis. Wavelets are adapted to local properties of functions to a larger extent than the Fourier basis. The adaptation is done automatically in view of the existence of a second degree of freedom: the localization in time (or space, if multivariate functions are considered).
The vertical axis in the next graphs denotes always the level, *i.e.*, the partition of the time axis into finer and finer resolutions. The advantage of this "multiresolution analysis" is that we can see immediately local properties of data and thereby influence our further analysis. There were attempts in the past to modify the Fourier analysis by partitioning the time domain into pieces and applying different Fourier expansions on different pieces. But the partitioning is always subjective. Wavelets provide an elegant and mathematically consistent realization of this intuitive idea [4].
In summary, wavelets offer a frequency/time representation of data that allows us time (respectively, space) adaptive filtering, reconstruction and smoothing.
Recall that a mother wavelet ψ is a function of zero h-th moment (*e.g.*, see [5], [6], [7], [8])

$$\int_{-\infty}^{+\infty} x^h \psi(x)dx = 0\,, \quad h \in \mathbf{N}. \tag{1}$$

From this definition, it follows that, if ψ is a wavelet whose all moments are zero, also the function $\psi_{jk}(x)$: $= 2^{j/2}\,\psi(2^j x - k)$ is a wavelet.
Now consider a wavelet ψ and a function φ such that $\{\{\varphi_{j_0 k}\}, \{\psi_{jk}\}, k \in \mathbf{Z}, j = 0, 1, 2, \ldots\}$ is a complete orthonormal system. In this case, a given signal $s(t)$, decomposed by wavelet (*i.e.*, CWT) is represented in the following detail function coefficients

$$d_{jk} = \int_{-\infty}^{+\infty} s(\tau) \cdot \frac{1}{\sqrt{2^j}} \psi\left(\frac{\tau - k}{2^j}\right) d\tau \tag{2}$$

and in the approximating scaling coefficients as follows

$$a_{j_0 k} = \int_{-\infty}^{+\infty} s(\tau) \cdot \varphi(\tau - k) d\tau \tag{3}$$

Note that, for any j, d_{jk} can be regarded, as a function of k. Consequently, if the signal $s(t)$ is a smooth function, then the relative details are zero, since, as said before, a wavelet has zero moments (for a detailed argumentation see [5]).
The sequence of spaces $\{V_j, j \in Z\}$, generated by φ is called a multiresolution analysis (*MRA*) of $L^2(R)$ if it satisfies the following properties

$$V_j \subset V_{j+1}, j \in Z \text{ and } \bigcup_{j \ge 0} V_j \text{ is dense in } L^2(R).$$

It follows that if $\{V_j, j \in Z\}$, is a *MRA* of $L^2(R)$, we say that the function φ generates a *MRA* of $L^2(R)$, and we call φ the father wavelet.
Besides, based on Parseval theorem, for any $s \in L^2(R)$, it follows that

$$s(t) = \sum_k a_{j_0 k}\varphi_{j_0 k}(t) + \sum_{j=j_0}^{j_1}\sum_k d_{jk}\psi_{jk}(t) \qquad (4)$$

The relation (4) is called a multiresolution expansion of *s*. This means that any $s \in L^2(R)$ can be represented as a series (convergent in $L^2(R)$), where a_k and d_{jk} are some coefficients, and $\{\psi_{jk}\}, k \in Z$, is a basis for W_j, where we define

$$W_j = V_{j+1} - V_j, \; j \in Z .$$

In (1) $\{\psi_{jk}(t)\}$ is a general basis for W_j. The space W_j is called resolution level of multiresolution analysis. In the following, by abuse of notation, we frequently write "resolution level *j*" or simply "level *j*". We employ these words mostly to designate not the space W_j itself, but rather the coefficients d_{jk} and the function ψ_{jk} "on the level *j*".
As the Fast Fourier Transform, the Discrete Wavelet Transform (DWT) is a fast and linear operation operating on a data array of length equal to a power of 2 and that transforms it in an array of equal length but numerically different. Both FFT and DWT could be considered as a transformation from the original dominion (*i.e.*, time) to a different dominion. In both the cases the functions used to operate the transformation form a Complete Orthonormal System (CONS). Unlike trigonometrical basis, which defines one only Fourier transform, infinite wavelet bases exist that differ for their localization in the dominion of the time and for their regularity.
A particular wavelet basis is characterized by numerical filters. In the present work it has been applied the filter proposed by Daubechies, which includes both wavelets strongly localized and wavelets strongly regular. A filter is characterized by *L* coefficients denoted as: $h_0, \ldots, h_{L-1}$.
We considered the Daubechies family of length $L = 4, h_0, \ldots, h_3$. The first step of wavelet transform was represented by the calculation of the following product

$$\boldsymbol{w}^{J-1} = W^J \boldsymbol{x}$$

where $\boldsymbol{x} \equiv \{x_0, x_1, \ldots, x_{N-1}\}$ is the vector of $N = 2^J$ data of which the wavelet transform have to be calculated. While $\boldsymbol{w}^{J-1}$ is the wavelet vector transform (of length *L*) after the first step of calculation; W^J is the *N* order wavelet transformation matrix

$$W^J = \begin{pmatrix} h_0 & h_1 & h_2 & h_3 & & & & & & \\ g_0 & g_1 & g_2 & g_3 & & & & & & \\ & & h_0 & h_1 & h_2 & h_3 & & & & \\ & & g_0 & g_1 & g_2 & g_3 & & & & \\ & & & & \ddots & & & & & \\ & & & & & & h_0 & h_1 & h_2 & h_3 \\ & & & & & & g_0 & g_1 & g_2 & g_3 \\ h_2 & h_3 & & & & & & & h_0 & h_1 \\ g_2 & g_3 & & & & & & & g_0 & g_1 \end{pmatrix}$$

The white elements are zero. It is important to observe the matrix structure. The first row generates the first element of convolution between $\boldsymbol{x}$ and the $\boldsymbol{h}$ filter.
Likewise the third, fifth..., and generally the odd rows of matrix generate the third, fifth..., element of convolution respectively.
The even rows generate the same type of convolution but with the filter $\boldsymbol{g}$ rather than $\boldsymbol{h}$. Filter $\boldsymbol{g}$ is called also the conjugated one of $\boldsymbol{h}$ and represents a pass-high filter.
It is uniquely determined by means of $\boldsymbol{h}$ as the following relation

$$g_k = (-1)^k h_{L-k-1}, \; k = 0, \ldots, L-1.$$

The **h** and **g** filters are also named *quadrature mirror filters* (QMF). Note that $\boldsymbol{g}$ is such to return null values if the vector of which we want to calculate the transform is sufficiently regular: in practical the coefficients g_k have $p = L/2$ null moments (in the following it will be esplicitate such a condition named "*p*-order approximation").
Therefore the output of the filter $\boldsymbol{h}$ is the vector $\boldsymbol{x}$ represented in a *coarse* shape, while the output of the filter $\boldsymbol{g}$ represents the *detail* that added to the *coarse* information allows to reconstruct the original vector.
We still notice that in the last two rows the coefficient h_2 and the correspondent high-pass filter g_2 are present due to the regularity conditions stated for the vector $\boldsymbol{x}$.
By means of the inverse transform it is possible to reconstruct the original vector $\boldsymbol{x}$ of length *N* by means of vectors of length *N/2* composed of

output of the convolution with the low-pass filter $\boldsymbol{h}$ and the high-pass filter $\boldsymbol{g}$.
The value of the elements of the vector filter $\boldsymbol{h}$ can be obtained by imposing the orthonormality condition for the matrix W^J as follows

$$h_0^2 + h_1^2 + h_2^2 + h_3^2 = 1$$
$$h_0 h_2 + h_1 h_3 = 0$$

and the "approximation condition of $p = L/2 = 2$ order"

$$g_0 + g_1 + g_2 + g_3 = 0$$
$$0g_0 + 1g_1 + 2g_2 + 3g_3 = 0$$

In the present work (*i.e.*, $L = 4$) the solution of condition is [5]

$$h_0 = \frac{1+\sqrt{3}}{4\sqrt{2}}$$
$$h_1 = \frac{3+\sqrt{3}}{4\sqrt{2}}$$
$$h_2 = \frac{3-\sqrt{3}}{4\sqrt{2}}$$
$$h_3 = \frac{1-\sqrt{3}}{4\sqrt{2}}$$

The DWT consists in applying the W^j matrix in hierarchical way to the vector $\boldsymbol{x}\left(W^J\right)$ of length $N = 2^J$, then to the *coarse* vector obtained by the convolution of $\boldsymbol{x}$ with the low-pass filter $\boldsymbol{h}$ (of $N/2=2^{J-1}$ length, with the W^{J-1} matrix), therefore still to the vector of $N/4$ length obtained from the next convolution with the filter $\boldsymbol{h}$, and so on until to a prefixed level J_0 or when the convolution with the low-pass filter supplies a single element.
The last procedure takes the name of pyramidal algorithm. In order to explain the procedure let us consider the case $N=16=2^4$.
Therefore the procedure is sensitized as follows

$$\begin{pmatrix} x_0 \\ x_1 \\ x_2 \\ x_3 \\ x_4 \\ x_5 \\ x_6 \\ x_7 \\ x_8 \\ x_9 \\ x_{10} \\ x_{11} \\ x_{12} \\ x_{13} \\ x_{14} \\ x_{15} \end{pmatrix} W^4 \rightarrow \begin{pmatrix} c_0^{(3)} \\ d_0^{(3)} \\ c_1^{(3)} \\ d_1^{(3)} \\ c_2^{(3)} \\ d_2^{(3)} \\ c_3^{(3)} \\ d_3^{(3)} \\ c_4^{(3)} \\ d_4^{(3)} \\ c_5^{(3)} \\ d_5^{(3)} \\ c_6^{(3)} \\ d_6^{(3)} \\ c_7^{(3)} \\ d_7^{(3)} \end{pmatrix} P \rightarrow \begin{pmatrix} c_0^{(3)} \\ c_1^{(3)} \\ c_2^{(3)} \\ c_3^{(3)} \\ c_4^{(3)} \\ c_5^{(3)} \\ c_6^{(3)} \\ c_7^{(3)} \\ d_0^{(3)} \\ d_1^{(3)} \\ d_2^{(3)} \\ d_3^{(3)} \\ d_4^{(3)} \\ d_5^{(3)} \\ d_6^{(3)} \\ d_7^{(3)} \end{pmatrix} W^3 \rightarrow \begin{pmatrix} c_0^{(2)} \\ d_0^{(2)} \\ c_1^{(2)} \\ d_1^{(2)} \\ c_2^{(2)} \\ d_2^{(2)} \\ c_3^{(2)} \\ d_3^{(2)} \end{pmatrix} P \rightarrow \begin{pmatrix} c_0^{(2)} \\ c_1^{(2)} \\ c_2^{(3)} \\ c_3^{(2)} \\ d_0^{(2)} \\ d_1^{(2)} \\ d_2^{(2)} \\ d_3^{(2)} \end{pmatrix} W^2 \rightarrow \begin{pmatrix} c_0^{(1)} \\ d_0^{(1)} \\ c_1^{(1)} \\ d_1^{(1)} \end{pmatrix} P \rightarrow \begin{pmatrix} c_0^{(1)} \\ c_1^{(1)} \\ d_0^{()1} \\ d_1^{(1)} \end{pmatrix} W^1 \rightarrow \begin{pmatrix} c_0^{(0)} \\ d_0^{(0)} \end{pmatrix}$$

where P is a permutation matrix of elements of vector $\mathbf{x}$ which orders all the coefficients of type "c" (*i.e.*, *coarse* coefficients) and type "d" (*i.e.*, *detail* coefficients). Practically the W^j matrix of order j acts on *coarse* coefficients of j level, while the *detail* coefficients of the same level are unchanged.
Therefore at the end the wavelet transform vector will be formed as following

$$\left(c_0^{(0)} d_0^{(0)} d_0^{(1)} d_1^{(1)} d_0^{(2)} d_1^{(2)} d_2^{(2)} d_3^{(2)} d_0^{(3)} d_1^{(3)} d_3^{(3)} d_4^{(3)} d_5^{(3)} d_6^{(3)} d_7^{(3)}\right)^T$$

where $c_0^{(0)}$ means the *coarse* coefficient obtained at the fourth step of wavelet transform, $d_0^{(0)}$ indicates the *detail* coefficient obtained on the same step, $d_0^{(1)}, d_1^{(1)}$ are the *detail* coefficients obtained at the third step of transform, the $d_k^{(2)}$, $k = 0,\ldots,3$ represent the *detail* coefficients obtained at the second step and finally $d_k^{(1)}, k = 0,\ldots,7$ the *detail* coefficients obtained at the first step of transform.
Since the procedure is based on orthogonal linear operations equally the WT will show the same feature.
For the calculation of the inverse transform, it will be sufficient to repeat the steps of the transform in the inverse order.
The performance of the WT algorithm is evaluated for real data. In this first experiment, we considered the real data shown in Fig. 5 as the input signal and applied the DWT to each signal decomposition level. The Fig. 9 below shows two singularities at 5th and 6th decomposition level.

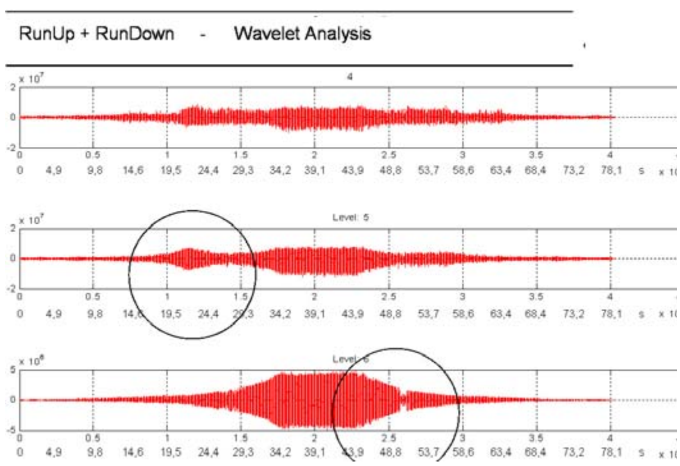

Fig. 9 RunUp + RunDown – Wavelet Analysis

6 Discussion and Conclusion

This work deals with the objective measurement of the gear noise, in particular with the analysis of the gear whine which represents transmission noises resulting from gears engaged in the torque flow, *i.e.* teeth engagement noise.

In this paper an “innovative” Wavelet’s approach is presented and the results on basic noise research of gear vibrations, obtained by using a “traditional” Fourier’s approach, were compared.

A brief theory of wavelet transforms and their effective computation method was showed. This is followed by the numerical results with related graphs.

From a deeper mechanical point of view, it is shown the ability of wavelet transform in order to detect and to localize, starting from the experimental data set of signals, the area where the energy and the entropy assume consistent value indicating the potential sliding and stress surface of tooth profile.

In fact a parallel main objective of this work for noise reduction is the use of vibration signature analysis procedures for health monitoring and diagnostics of a gear transmission system .

In order to approach such a problem, probably, we have to modify the pressure angle and corresponding arches of circumference, constituting the tooth profile, until the first derivative. The first results are interesting and show that if we design a line of action that fulfils the kinematical behavior requirements of the gear pair it will be much easier, by applying the wavelets, to ensure the kinematical quality of the designed gear pair.

Then the proposed methodology will be tested in order to investigate deeper on the regularity of the line of action.

The objective is to calculate the shape of the required modified hobbing tools and to show that the generation process will be no more complicated than that used currently for the production of standard gears [9][10][11].

The work suggests some directions for future investigations:

- reduction of undercutting and interference problem
- reduction of slipping speeds [12]
- increase loading capacity
- increase rigidity of toothing
- reduction of noise and radial forces [13].

Finally, in order to improve the reliability of the proposed method, investigation will be conducted further on a wider case-wise as well as to verify this design, a series of numerical simulations will be carried out using the boundary element method (BEM), and the results will be confirmed with subsequent laboratory testing.

In this case the application of Wavelet Transform is also able for the identification and quantification of gear noise based on the numerically generated vibration signal.

In fact a subsequent goal of this research work is the use of noise-vibration signature analysis procedures for health monitoring and diagnostics of a gear transmission system [13].

Important advancements in preventive maintenance of gear transmission systems are currently being sought for the development of an accurate machine health diagnostic system. Such a diagnostic system would use vibration or acoustic signals from the gear transmission system for

- rapid on-line evaluation of gear wear or damage status
- prediction of remaining gear life.

Such health diagnostic capabilities would be essential for effective machine event/life management and advance warning before critical component failures.

Finally, in order to reduce the gear noise we have to examine another requirement: the shape of teeth necessary for the speed ratio to remain constant during an increment of rotation; this behavior of the contacting surfaces (*i.e.*, the teeth flanks) is known as *conjugate action*.

References:

[1] Rader C.M., Discrete Fourier Transform when the Number of Data Samples is Prime", Proc. IEEE, vol. 56, pp. 1107-1108, June 1968

[2] Genta G., A Fast Modal Technique for the Computation of the Campbell Diagram of Multi-Degrees of Freedom Rotors, Journal of Sound and Vibration, 155(3), 1992

[3] Harris F.J., On the use of window for harmonic analysis with the discrete Fourier transform, Proc. IEEE, vol. 66, pp. 51-83, Jan. 1978

[4] Härdle W., Kerkyacharian G., Picard D. and Tsybakov A., *Lecture Notes in Statistics* - Wavelets, Approximation, and Statistical Applications, Springer, 1998

[5] Daubechies I., *Ten Lectures on Wavelets*, SIAM, 1992

[6] Antoniadis A., Oppenheim G., Lecture notes in Statistics - Wavelets and Statistics, Springer, 1995

[7] Kaiser G., A Friendly Guide to Wavelets, Birkhäuser, 1999

[8] Anthony, T**.,** *Computational Signal Processing with Wavelets*, Birkhäuser, Boston, 1998

[9] C. Lee, H.H. Lin, F.B. Oswald and D.P. Towsend, Influence of linear profile modification and loading conditions on the dynamic tooth load and stress of high-contact-ratio spur gears, ASME Journal of Mechanical Design, Vol. 113, pp. 473-480 1991.

[10] C. Lee, H.H. Lin, F.B. Oswald and D.P. Towsend, Computer-aided design of high-contact-ratio gears for minimum dynamic load and stress, ASME Journal of Mechanics Design, Vol. 115, pp. 171-178, 1993.

[11] C. Lee, H.H. Lin, F.B. Oswald and D.P. Towsend Lee, Effect of contact ratio on spur gear dynamic load with no tooth profile modifications, ASME Journal of Mechanics Design, Vol. 118, pp. 439-443, 1996.

[12] A.L. Kapelevich and R.E. Kleiss , Direct Gear Design for Spur and Helical Involute Gears, Gear Technology, Sept.-Oct., pp. 29-35, 2002.

[13] F.K. Choy, D.H. Mugler and J. Zhou, Damage Identification of a Gear Transmission Using Vibration Signatures, ASME Trans. J. Mechanical Design, Vol. 125 , pp. 394-403, 2003.